Carbohydrate Polymers 113 (2014) 108–114

Contents lists available at ScienceDirect

Carbohydrate Polymers

journal homepage: www.elsevier.com/locate/carbpol

Acidic ionic liquid catalyzed crosslinking of oxycellulose with chitosan for advanced biocomposites

Yonghui Zhou[a,b], Mizi Fan[a,b,*], Xiaolin Luo[a,c], Liulian Huang[a], Lihui Chen[a,*]

[a] College of Material Engineering, Fujian Agriculture and Forestry University, Fuzhou 350002, China
[b] School of Engineering and Design, Brunel University, Middlesex UB8 3PH, UK
[c] Key Laboratory of Biofuel, Chinese Academy of Sciences, Qingdao Institute of Bioenergy and Bioprocess Technology, Qingdao 266101, China

ARTICLE INFO

Article history:
Received 22 March 2014
Received in revised form 15 June 2014
Accepted 20 June 2014
Available online 10 July 2014

Keywords:
Chitosan
Oxycellulose
Ionic liquids
Chitosan-crosslinked oxycellulose composite

ABSTRACT

This paper presents a novel environmentally friendly production of chitosan-crosslinked oxycellulose films by using ionic liquids (AmimCl and $SmimHSO_4$). The effect of reaction parameters on chitosan contents and mechanical properties of chitosan-crosslinked oxycellulose films was also investigated. The results revealed that appropriate $SmimHSO_4$ dosage and reaction time were 5% and 2 h respectively. FTIR analysis of chitosan-crosslinked oxycellulose film suggested that the chitosan was crosslinked with oxycellulose through the reaction between the amino groups in chitosan and the aldehyde groups in oxycellulose, and the results of XPS analysis further confirmed the reaction between both polysaccharides. SEM images suggested that the developed chitosan-crosslinked oxycellulose films had a smooth and compact structure, and a highly inhibitory effect against the bacteria of *Escherichia coli* and *Staphylococcus aureus*. The developed materials and technologies could be further formulated for the production of various antimicrobial and biomedical products or water treatment membranes.

1. Introduction

Polysaccharides, such as cellulose (poly β-(1, 4)-D-glucose) and chitosan (poly β-(1, 4)-2-amino-2-deoxy-D-glucose), are widely used in the fields of biotechnology, cosmetics, waste water treatment, membrane separation, food package, pharmaceuticals and drug carriers, due to the abundance of resources, excellent physical, chemical and biological properties, and eco-friendly characteristic of biomass (Liu & Bai, 2005; Muzzarelli, 2010, 2011; Pillai, Paul, & Sharma, 2009). The applications have been further extended when ionic liquids (ILs) are developed to dissolve the natural polymers directly without derivatization reactions, which are considered as green solvents replacing traditional volatile organic solvents in various processing and synthesis industries (Chen, Xiao, Zhou, Wu, & Wu, 2012; Chen, Xu, Li, Wang, & Zhang, 2011; Ma, Hsiao, & Chu, 2011). The ILs dissolved cellulose, chitin and chitosan solutions could be used to fabricate fibers (Li et al., 2012; Ma, Qin, Li, & He, 2013), gels (Kunchornsup & Sirivat, 2014), membranes (Setoyama, Kato, Yamamoto, & Kadokawa, 2013) and microspheres (Liu et al., 2012).

Recently, cellulose and chitosan were combined together to prepare cellulose–chitosan composites through the co-dissolution of both biopolymers in ILs (Ma, Zhang, He, & Sun, 2012; Ma et al., 2011; Stefanescu, Daly, & Negulescu, 2012; Sun, Peng, Ji, Chen, & Li, 2009), which seems to be a direct and efficient way to develop a composite by taking advantage of both biopolymers of cellulose and chitosan, especially the former giving mechanical strength and the latter antibacterial properties. However, the previous researches have indicated some shortages, including: (1) the chitosan could not be dissolved in ILs as efficiently as cellulose due to the presence of amino groups in its macromolecular chains (Ma et al., 2012), (2) the antibacterial ability of these hybrid composite films was limited (Shih, Shieh, & Twu, 2009) and (3) the chitosan embedded in cellulose would be leached if these films were used to treat water as a water purification membrane (Ma et al., 2011). Therefore, the chemical modifications of cellulose and chitosan to promote the crosslinking reaction between and within the chitosan and cellulose are in particular needed.

Current conversion of the 2,3-dihydroxyl groups of glucose in cellulose chain into dialdehyde groups by periodate oxidation and further crosslinking chitosan with cellulose, which is the reaction between the generated aldehyde groups in cellulose and amino groups in chitosan, is a classic approach of crosslinking reaction

* Corresponding authors at: College of Material Engineering, Fujian Agriculture and Forestry University, Fuzhou 350002, China. Tel. +86 59183715175; fax: +86 59183715175.
E-mail addresses: fafuclh@163.com (L. Chen), Mizi.Fan@brunel.ac.uk (M. Fan).

http://dx.doi.org/10.1016/j.carbpol.2014.06.081
0144-8617/

(imine formation reaction) (e.g. Hou, Liu, Liu, Duan, and Bai (2009); Janjic, Kostic, Vucinic, Dimitrijevic, & Popovic, 2009). The crosslinking reaction could also take place between carboxymethylated chitosan and oxidized carboxymethyl cellulose (Fan et al., 2013). However, to perform such reactions, the volatile and corrosive inorganic solvents have to be used, giving rise to waste water which is difficult to be recovered.

This paper presents a novel and green approach of generating crosslinking reactions between chitosan and oxycellulose, through the use of 1-allyl-3-methylimidazolium chloride (AmimCl) IL as the solvent of oxycellulose and the 1-sulfobutyl-3-methylimidazolium hydrogen sulfate (SmimHSO$_4$) IL as the catalyst of the reaction. This novel development is to formulate advanced cellulose–chitosan based composites without using volatile, toxic and corrosive solvents. The optimum parameters of the crosslinking reaction have been determined in terms of their effects on the mechanical properties and the chitosan contents of chitosan-crosslinked oxycellulose films. The reaction was also verified by the Fourier transform infrared spectroscopy (FTIR) and X-ray photoelectron spectroscopy (XPS). The morphology and antibacterial properties of the crosslinked composite films were characterized by the scanning electron microscopy (SEM) and antibacterial test.

2. Materials and methods

2.1. Materials

Cellulose was obtained from the Nanping Papermaking Company (Nanping City, China). Chitosan (deacetylation degree > 90%) was purchased from the Shandong Aokang Biotech Co. Ltd. (Jinan City, China). Both cellulose and chitosan were firstly dried at 80 °C for 12 h to remove the contained water and then used without any other purification. AmimCl and SmimHSO$_4$ were purchased from the Lanzhou Institute of Chemical Physics (Lanzhou City, China) and used as received.

2.2. Periodate oxidation of cellulose fibers

The dried cellulose (4 g) and sodium periodate (0.03 mol/L, 100 mL) were initially mixed in a round-bottomed flask and the mixtures were stirred at 35 °C for 120 min in the absence of light. After the oxidization, the cellulose fibers were washed thoroughly with deionized water to remove oxidant. The fibers were then dried in the atmosphere overnight at room temperature before crosslinking reactions. The content of aldehyde groups in the oxidized cellulose was determined according to a methodology reported by Hou et al., 2009 and calculated as 1170 μmol/g.

2.3. Preparation of chitosan-crosslinked oxycellulose films

Preparation procedure for chitosan-crosslinked oxycellulose films can be described as follows: A uniform and transparent 2% oxycellulose-AmimCl solution was firstly prepared in a round-bottomed flask; the chitosan (chitosan:oxycellulose = 1:1) was then added to the solution. Meanwhile, the required quantity of SmimHSO$_4$, namely 0% (0/25, SmimHSO$_4$ to AmimCl), 4% (1/25), 5% (1/20), 6.67% (1/15) and 10% (1/10)), was added as a catalyst for the reaction between oxycellulose and chitosan (Fig. 1). The reaction process was carried out at room temperature under intensive agitation. After the reaction, the resulted solution was centrifugalized for 20 min at a speed of 4000 r/min to remove the excess chitosan in the solution. The clear solution was finally developed and then casted onto an acryl slide with a spreading coater (GBC-A4, GIST, Korea) to form chitosan-crosslinked oxycellulose composite films. The formed films were immediately immersed in an ethanol/water solution (50/50, v/v) to coagulate and simultaneously remove AmimCl and HmimSO$_4$. The formulated composite films were finally dried in the atmosphere overnight at room temperature before testing. As a control, the regenerated oxycellulose films were prepared in parallel. It is worthy to note that in this study, the reaction system was designed not to be able to dissolve chitosan in order to formulate the chitosan grafted cellulose films. If the chitosan was soluble in the ionic liquids, it would be impossible to differentiate the origin of the composition of chitosan (dissolution or crosslinking) from that of oxycellulose in the resultant composite films. Therefore, there is no chitosan film as a control.

2.4. Characterization of chitosan-crosslinked oxycellulose films

2.4.1. Nitrogen and chitosan contents analysis

Nitrogen content in the chitosan-crosslinked oxycellulose films was mainly determined using a Kjeltec analyzer (KDN-B, Shanghai Xinjia Electrics Co. Ltd., China) and calculated as follows (United States Patent, 2001), although the relative quantity of the nitrogen content was also presented from the XPS examination:

$$N = \frac{(T - B) \times N' \times 14.007 \times 100\%}{w}$$

where the T and B are the volume of hydrochloric acid solution (HCl) used in sample and blank titration respectively, in milliliters; N' is the concentration of standard HCl solution, in mol/L; w is the weight of tested sample, in grams.

The chitosan content crosslinked with oxycellulose was calculated with the following formula (Hou et al., 2009):

$$C = \frac{N\%}{14.007} \times 166.74$$

2.4.2. Mechanical properties analysis

According to the ASTM D 882-02 standard (ASTM, 2002), films were cut into strip-shaped specimens of 15 mm width and 50 mm length. The tensile strengths of all the specimens were determined using a testing machine (CMT 6104, Shenzhen SANS Test machine Co. Ltd., China). For each sample, the tensile strength reported is the average of six measurements.

2.4.3. Fourier transform infrared spectroscopy (FTIR) analysis

The FTIR spectra of oxycellulose and chitosan-crosslinked oxycellulose films were measured with wave numbers ranging from 4000 to 400 cm^{-1} by using a Fourier transform infrared spectrometer (Thermo-Nicolet AVATAR 380, USA) and using 50 scans with a resolution of 4 cm^{-1}.

2.4.4. X-ray photoelectron spectroscopy (XPS) analysis

XPS analysis was carried out with an ESCALAB 250 X-ray photoelectron spectrometer (Thermo Fisher Scientific, US) equipped with a monochromatic Al-Kα X-ray source. For data acquisition, the survey scans and high-resolution scans were collected using the passing energy of 150 eV and 30 eV, respectively.

2.4.5. Scanning electron microscopy (SEM) analysis

The surface and cross section morphologies of oxycellulose and chitosan-crosslinked oxycellulose films were imaged by SEM (FEI NOVA NANO SEM, USA) at 3.0 kV. All samples were conductively plated with gold by sputtering for 20 s before imaging.

2.4.6. Antibacterial test

Escherichia coli ATCC 25922 (*E. coli*) and *Staphylococcus aureus* ATCC 25923 (*S. aureus*) were selected as the bacteria for determining the antibacterial properties of the developed composite films. All the samples were cut into 6 mm-diameter films and sterilized at

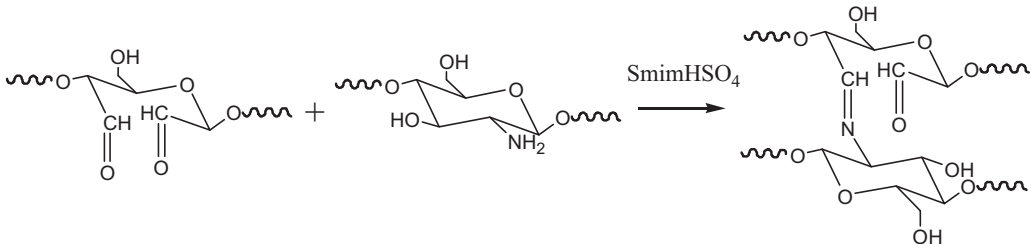

Fig. 1. Crosslinking reaction between oxycellulose and chitosan.

121 °C for 20 min. The sterilized films were then placed on the central part of petri dishes that contained 20 mL of nutrient agar with 10^7 CFU/mL *E. coli* and *S. aureus* respectively. The dishes containing the composite films and bacteria were then incubated at 37 °C for 24 h. The inhibition zone was then measured.

3. Results and discussion

3.1. Reaction between chitosan and oxycellulose

The effect of $SmimHSO_4$ dosage on the nitrogen and chitosan contents in chitosan-crosslinked oxycellulose composite films was shown in Fig. 2a. It can be seen that the nitrogen and chitosan contents in the chitosan-crosslinked oxycellulose films without adding $SmimHSO_4$ in reaction system were very low, only 0.20% and 2.4% respectively. The nitrogen and chitosan contents in the films increased almost linearly with an increase of $SmimHSO_4$ until 5%, from 0.20% to 0.69% for the nitrogen content and from 2.4% to 8.3% for the chitosan content. However, the level of the increase reduced significantly when the $SmimHSO_4$ dosage continued to increase more than 5%. This may be due to the favorable acidic environment promoting the reaction between amino groups in chitosan and aldehyde groups in oxycellulose (Santos, Dockal, & Cavalheiro, 2005): when there was no $SmimHSO_4$ in the reaction system, which tends to be a neutral system, the chitosan and oxycellulose may not be able to react efficiently with each other due to the poor nucleophilicity of amino groups; when the Brønsted acidic ionic liquid $SmimHSO_4$ was added to the system, the nucleophilicity of chitosan increased, which facilitated the reaction between chitosan and oxycellulose and finally led to an increase of nitrogen and chitosan contents in chitosan-crosslinked oxycellulose films.

Fig. 2b shows the effect of reaction time on nitrogen and chitosan contents in the chitosan-crosslinked oxycellulose films, when the $SmimHSO_4$ dosage was set at 5%. It was observed that there was no nitrogen element existed in oxycellulose films at the beginning of the reaction (reaction time = 0 min). Nitrogen and chitosan contents in the films increased with the increase of reaction time. While the contents of both nitrogen and chitosan rapidly increased linearly in the first hour, from 0% to 0.58% for the former and from 0% to 6.9% for the latter, their increases were stabilizing after about 1.5 h as the reaction between amino groups in chitosan and the limited aldehyde groups in oxycellulose may become saturated.

The results from XPS examination have also been summarized in Table 1. However, it must be noted that the values were the relative quantities over C, N and O elements, but without including the H element. The measurement is also only for the elemental composition of the surface. It can be seen that the measured atomic concentration was not comparable to the theoretical atomic ratios of the measured material (Table 1), e.g. for the N element, only about 4% of the measured values compared to about 8% of the theoretically calculated values. Nevertheless, a comparison of

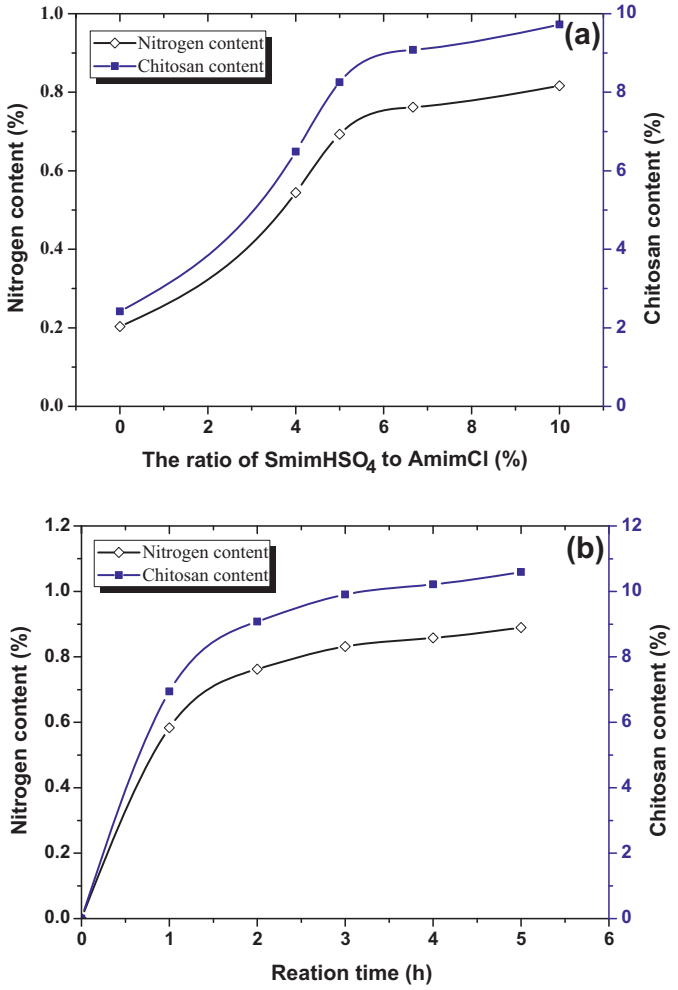

Fig. 2. Effect of $SmimHSO_4$ dosage (a) and reaction time (b) on nitrogen and chitosan contents in chitosan-crosslinked oxycellulose films.

Table 1
C, O and N elements of chitosan and chitosan-crosslinked oxycellulose film measured by XPS.

Material	Area percentage of XPS scan (at%)						
	C_{1s} scan A	C_{1s} scan B	C_{1s} scan C	O_{1s}	N_{1s} scan A	N_{1s} scan B	N_{1s} scan C
Chitosan	28.76	29.48	10.3	27.51	1.1	2.86	–
Chitosan-crosslinked oxycellulose film	29.33	26.54	9.02	31.85	0.49	2.56	0.22

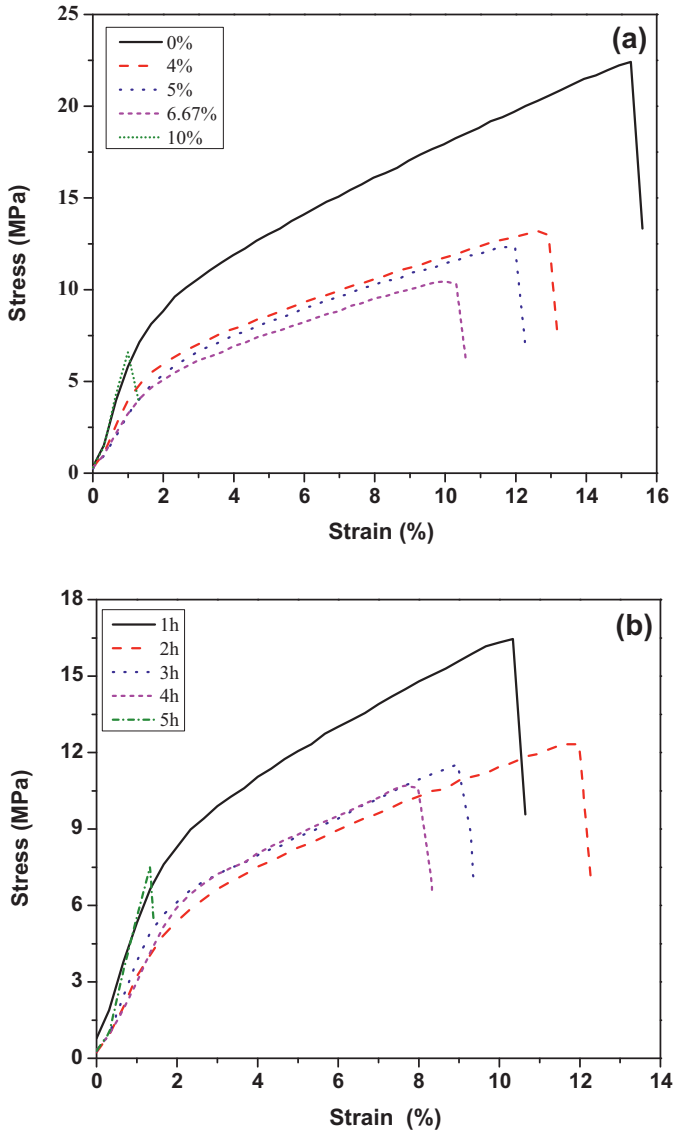

Fig. 3. Effect $SmimHSO_4$ dosage (a) and reaction time (b) on the stress–strain behavior of chitosan-crosslinked oxycellulose films.

the relative quantities of the N elements within the chitosan and chitosan-crosslinked oxycellulose composite films was also able to indicate the crosslinking reactions taking place between chitosan and oxycellulose, by considering that there was only about 3.3% N element in the composite films (Table 1).

3.2. Mechanical properties

Fig. 3 shows the stress–strain of chitosan-crosslinked oxycellulose films. The chitosan-crosslinked oxycellulose films prepared without the addition of $SmimHSO_4$ (0%) had the highest tensile strength and elongation at break, which were calculated as 22.4 MPa and 15.6% respectively. With the increase of $SmimHSO_4$ dosage or reaction time, the tensile strength and the elongation at break of the chitosan-crosslinked oxycellulose films decreased. This may mainly be due to the degradation of oxycellulose during the reaction process. After dissolution in AmimCl, the inter- and intro-molecular hydrogen bonding in the oxycellulose may have been broken (Hong et al., 2012), which could lead to the gradual reduction in the strength of oxycellulose itself and hence an overall degradation of the composite system, especially under intense

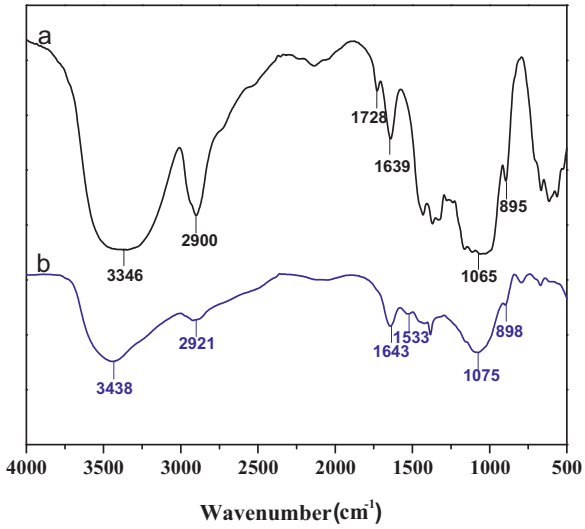

Fig. 4. FTIR spectra of oxycellulose (a) and chitosan-crosslinked oxycellulose (b) films.

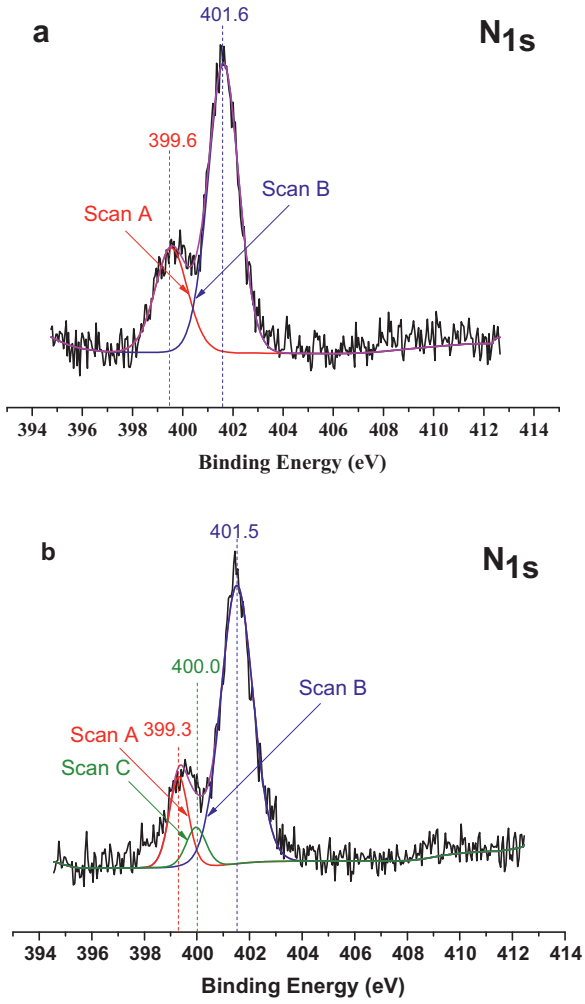

Fig. 5. XPS spectra of the N_{1s} peak of chitosan (a) and chitosan-crosslinked oxycellulose films (b).

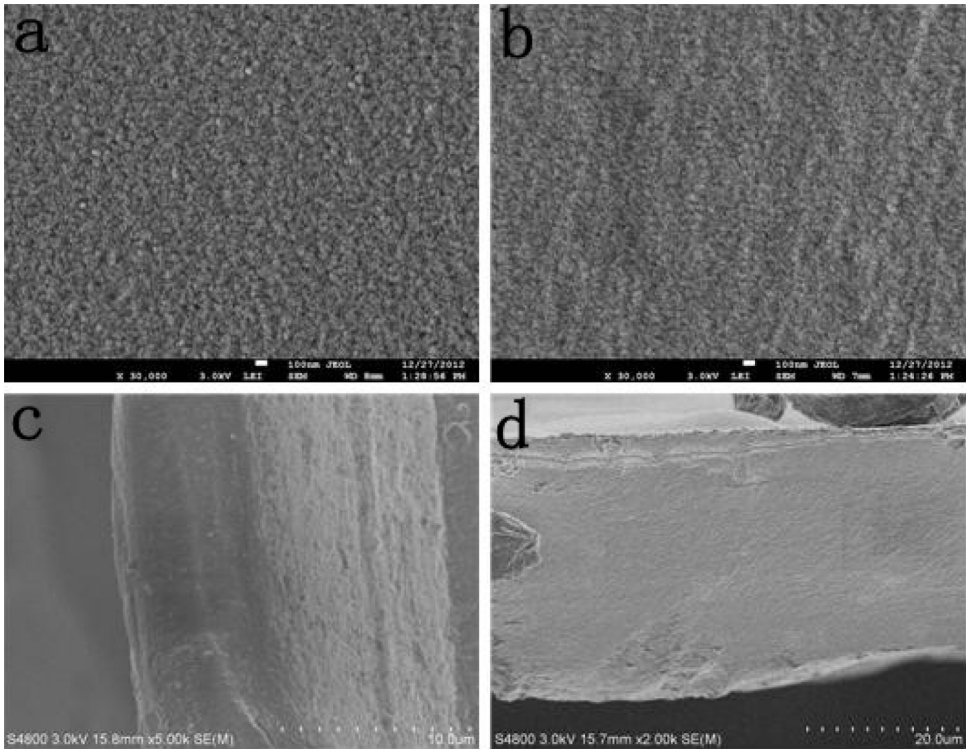

Fig. 6. SEM images of surface (a, b) and cross section (c, d) of oxycellulose and chitosan-crosslinked oxycellulose films.

agitation in an acidic environment. It is apparent that although with the increase of $SmimHSO_4$ dosage or reaction time, more chitosan were crosslinked with oxycellulose, the mechanical performance of the crosslinked films could not be enhanced due to the inferior mechanical properties of the treated oxycellulose (Pillai et al., 2009).

By virtue of the continuous decrease of mechanical properties (Fig. 3) but the increase of nitrogen and chitosan contents (Fig. 2) of the crosslinked films with the increase of $SmimHSO_4$ dosage and reaction time, a combination of the $SmimHSO_4$ dosage and reaction time of 5% and 2 h was used to prepare chitosan-crosslinked oxycellulose films for other analyses.

3.3. FTIR spectra analysis

Fig. 4 demonstrates the FTIR spectra of oxycellulose and chitosan-crosslinked oxycellulose composite films. The adsorption peaks at 1065 cm^{-1} and 1075 cm^{-1} in both spectra corresponded to the C—O—C dissymmetry stretching vibration, while the peaks at 895 cm^{-1} and 898 cm^{-1} referred to β-(1–4) stretching vibration (Lan, Liu, Yue, Sun, & Kennedy, 2011). This indicated that the main chains of oxycellulose did not change after crosslinked with chitosan. It is interesting that the peak at 1728 cm^{-1} assigned to carbonyl groups in oxycellulose (Da Roz et al., 2010) did not come up in spectrum (b), which indicated that the aldehyde groups in oxycellulose may have reacted with the amino groups in chitosan. This result was confirmed by the evidence of a new peak at 1533 cm^{-1} in spectrum (b), which could be attributed to N—H in plane deformation coupled with C—N stretching of the crosslinked chitosan (Amaral, Granja, & Barbosa, 2005). In addition, the peak for hydrogen-bonded —OH stretching at 3346 cm^{-1} in spectrum (a) has shifted to 3438 cm^{-1} in spectrum (b) due to the contribution of the —NH stretching after the crosslinking reaction. A similar phenomenon could also be observed for the shift of the peak of carboxyl stretching at 1639 cm^{-1} in spectrum (a) to a higher frequency in spectrum (b) (1643 cm^{-1}). This may be due to the overlapping of the C=N characteristic vibrations of imines with C=O stretching (Guan, Xiao, Sullivan, & Zheng, 2007; Jin, Wang, & Bai, 2009), which has also confirmed the reaction between chitosan and oxycellulose.

3.4. XPS spectra analysis

The high-resolution N_{1s} spectra of chitosan (a) and chitosan-crosslinked oxycellulose (b) films are shown in Fig. 5. The N_{1s} spectrum of chitosan was deconvoluted into two binding energy peaks at 399.6 eV (N_{1s} scan A) and 401.6 eV (N_{1s} scan B). Considering the chemical structure of chitosan, the first peak was assigned to —N—C=O (amide) and —NH_2 (amine), and the second peak was due to —NH_3^+ (protonated amine) (Amaral et al., 2005; Deng et al., 2011; Ignatova, Manolova, Markova, & Rashkov, 2009). However, these three components, amine, amide and protonated amine, have also been reported with three binding energy peaks at 399.5 eV, 400.5 eV and 401.9 eV, respectively (Huang, Cao, & Liu, 2012), which are in agreement with that of the chitosan film cast from a hydrochloric acid solution (Lawrie et al., 2007). The above difference might be resulted from the variation in the degree of deacetylation of chitosans.

Both of these two peaks of N_{1s} scan A and N_{1s} scan B in spectrum (a) could be seen in spectrum (b) with a little shift to a lower frequency. However, there was a new binding energy peak coming up at 400.0 eV (N_{1s} scan C) in spectrum (b), which could be attributed to N=C originated from the reaction between chitosan and oxycellulose. Moreover, the significant reduction in the area covered under spectra A in (b), about half that in (a), and the presence of new peak in spectrum (b) also indicated the crosslinking reaction between chitosan and oxycellulose (Table 1). The XPS results are also consistent with the FTIR results discussed in the previous section, which again confirm the crosslinking reactions existed between chitosan and oxycellulose.

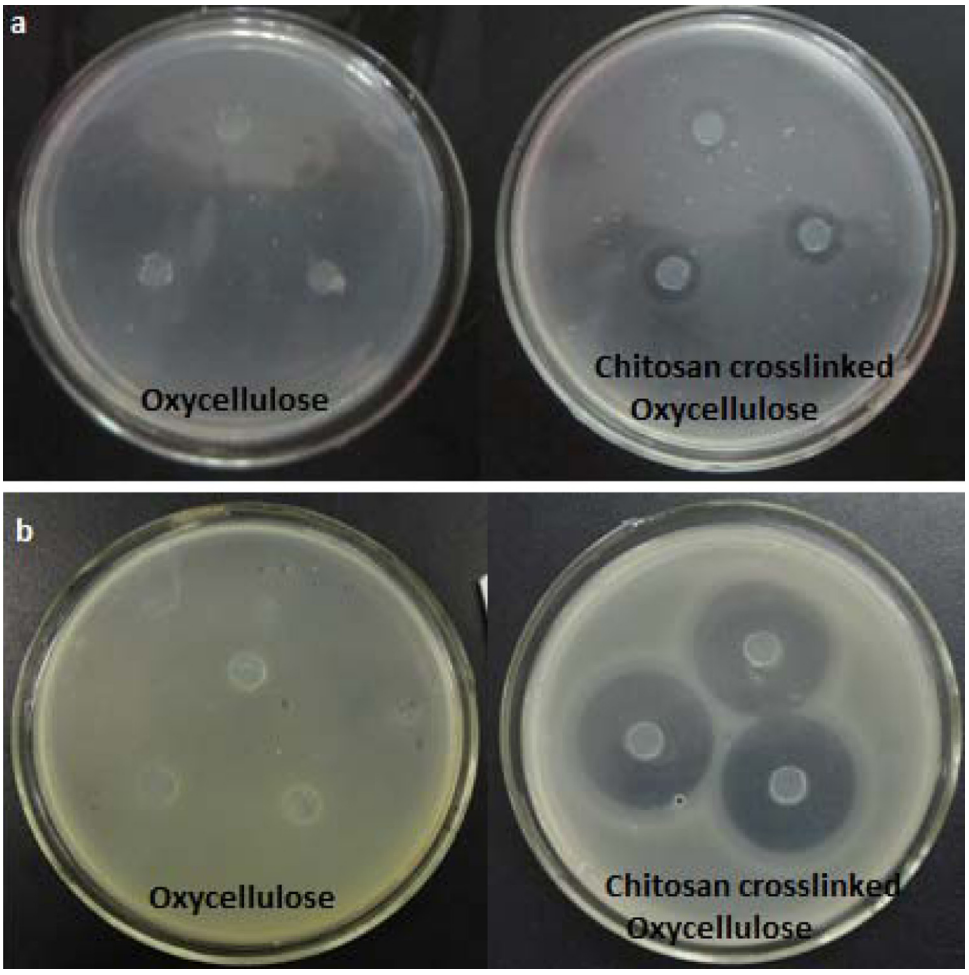

Fig. 7. The antibacterial activity of oxycellulose and chitosan-crosslinked oxycellulose films against *E. coli* (a) and *S. aureus* (b).

3.5. Morphology observation

The SEM images of surface and cross section of oxycellulose and chitosan-crosslinked oxycellulose films were shown in Fig. 6a–d. Overall, both oxycellulose and chitosan-crosslinked oxycellulose films with 30,000 times magnification displayed a smooth and uniform surface structure (image a and b). This was different from cellulose–chitosan blend membranes (Liu & Bai, 2005; Wu et al., 2010), which exhibited uneven surface and porous structure. Moreover, since an ethanol–water solution (50/50, v/v) was used as the coagulant in the film-forming process, phase inversion occurred immediately once the polymer solutions were immersed in the coagulant. A scrutiny of images indicated that both the surface (image b) and cross-section structure (image d) of the chitosan-crosslinked oxycellulose films were slightly smoother and denser than those of oxycellulose films (image a and c). The possible reason was that compared with oxycellulose films, there might be more hydrogen bonding existed among $-NH_2$,–C=O and –OH groups in chitosan-crosslinked oxycellulose molecules, which facilitated the drying process after regeneration process.

3.6. Antibacterial test

The antimicrobial properties of oxycellulose and chitosan-crosslinked oxycellulose films exposed to *E. coli* and *S. aureus* were shown in Fig. 7. It is evident that the oxycellulose films had no inhibitory effect against both bacteria of *E. coli* and *S. aureus*, while the chitosan-crosslinked oxycellulose films clearly exhibited an effective antimicrobial ability against both *E. coli* and *S. aureus*. It therefore demonstrates that instead of losing its antibacterial property after crosslinking with oxycellulose, the chitosan has provided the crosslinked oxycellulose films with antibacterial ability against both Gram-negative bacteria (*E. coli*) and Gram-positive bacteria (*S. aureus*).

4. Conclusions

New chitosan-crosslinked oxycellulose films were successfully developed using ionic liquids. On balance of nitrogen and chitosan contents and mechanical properties of chitosan-crosslinked oxycellulose films, the appropriate $SmimHSO_4$ dosage and reaction time were determined as 5% and 2 h respectively. The reaction of chitosan and oxycellulose within chitosan-crosslinked oxycellulose films resulted in half spectrum area of the binding energy 399.6 eV and new binding energy peak at 400.0 eV in XPS spectrum, compared to those of oxycellulose films. The chitosan-crosslinked oxycellulose films had the similar or better surface and compact structure compared to oxycellulose films. In addition, the crosslinking of chitosan with oxycellulose gave rise to excellent antibacterial ability against *E. coli* and *S. aureus*. The development of the chitosan-crosslinked oxycellulose has provided a basis for possible development of various antimicrobial and biomedical products or water treatment membranes in future.

Acknowledgements

The authors gratefully acknowledge the financial supports from the Doctoral Fund of Ministry of Education of China

(No. 20123515120018), National Nature Science Foundation of Fujian Province (No. 2013J05041), Open Foundation of the Chinese Academy of Sciences Key Laboratory of Biofuels (No. CASKLB201308), and Open Foundation of the State Key Laboratory of Pulp and Paper Engineering (South China University of Technology, No. 201222).

References

Amaral, I. F., Granja, P. L., & Barbosa, M. A. (2005). Chemical modification of chitosan by phosphorylation: An XPS, FT-IR and SEM study. *Journal of Biomaterials Science*, *16*, 1575–1593.

ASTM. (2002). Standard test method for tensile properties of thin plastic sheeting. Standard designation: D882-02. In *Annual books of ASTM*. Philadelphia: ASTM.

Chen, Q., Xiao, W. J., Zhou, L. L., Wu, T. H., & Wu, Y. (2012). Hydrolysis of chitosan under microwave irradiation in ionic liquids promoted by sulfonic acid-functionalized ionic liquids. *Polymer Degradation and Stability*, *97*, 49–53.

Chen, Q. T., Xu, A. R., Li, Z. Y., Wang, J. J., & Zhang, S. J. (2011). Influence of anionic structure on the dissolution of chitosan in 1-butyl-3-methylimidazolium-based ionic liquids. *Green Chemistry*, *13*, 3446–3452.

Da Roz, A. L., Leite, F. L., Pereiro, L. V., Nascente, P. A. P., Zucolotto, V., Oliveira, O. N., Jr., et al. (2010). Adsorption of chitosan on spin-coated cellulose films. *Carbohydrate Polymers*, *80*, 65–70.

Deng, H., Wang, X., Liu, P., Ding, B., Du, Y., Li, G., et al. (2011). Enhanced bacterial inhibition activity of layer-by-layer structured polysaccharide film-coated cellulose nanofibrous mats via addition of layered silicate. *Carbohydrate Polymers*, *83*, 239–245.

Fan, L., Tan, C., Wang, L., Pan, X., Cao, M., Wen, F., et al. (2013). Preparation, characterization and the effect of carboxymethylated chitosan–cellulose derivatives hydrogels on wound healing. *Journal of Applied Polymer Science*, *128*, 2789–2796.

Guan, Y., Xiao, H., Sullivan, H., & Zheng, A. (2007). Antimicrobial-modified sulfite pulps prepared by in situ copolymerization. *Carbohydrate Polymers*, *69*, 688–696.

Hong, F., Guo, X., Zhang, S., Han, S., Yang, G., & Jonsson, L. (2012). Bacterial cellulose production from cotton-based waste textiles: Enzymatic saccharification enhanced by ionic liquid pretreatment. *Bioresource Technology*, *104*, 503–508.

Hou, Q. X., Liu, W., Liu, Z. H., Duan, B., & Bai, L. L. (2009). Characteristics of antimicrobial fibers prepared with wood periodate oxycellulose. *Carbohydrate Polymers*, *74*, 235–240.

Huang, P., Cao, M., & Liu, Q. (2012). Adsorption of chitosan on chalcopyrite and galena from aqueous suspensions. *Colloids and Surfaces A: Physicochemical and Engineering Aspects*, *409*, 167–175.

Ignatova, M., Manolova, N., Markova, N., & Rashkov, I. (2009). Electrospun nonwoven nanofibrous hybrid mats based on chitosan and PLA for wound-dressing applications. *Macromolecular Bioscience*, *9*, 102–111.

Janjic, S., Kostic, M., Vucinic, V., Dimitrijevic, S., & Popovic, K. (2009). Biologically active fibers based on chitosan-coated lyocell fibers. *Carbohydrate Polymers*, *78*, 240–246.

Jin, X., Wang, J., & Bai, J. (2009). Synthesis and antimicrobial activity of the Schiff base from chitosan and citral. *Carbohydrate Research*, *344*, 825–829.

Kunchornsup, W., & Sirivat, A. (2014). Thermo-electromechanical responses of 1-butyl-3-methylimidazolium chloride ionic liquid-cellulose gel. *Journal of Polymer Research*, *21*(369), 1–9.

Lan, W., Liu, C. F., Yue, F. X., Sun, R. C., & Kennedy, J. F. (2011). Ultrasound-assisted dissolution of cellulose in ionic liquid. *Carbohydrate Polymers*, *86*, 672–677.

Lawrie, G., Keen, G., Drew, B., Chandler-Temple, A., Rintoul, L., Fredericks, P., et al. (2007). Interactions between alginate and chitosan biopolymers characterized using FTIR and XPS. *Biomacromolecules*, *8*, 2533–2541.

Li, L., Yuan, B., Liu, S., Yu, S., Xie, C., Liu, F., et al. (2012). Preparation of high strength chitosan fibers by using ionic liquid as spinning solution. *Journal of Materials Chemistry*, *22*, 8585–8593.

Liu, C. L., & Bai, R. B. (2005). Preparation of chitosan/cellulose acetate blend hollow fibers for adsorptive performance. *Carbohydrate Polymers*, *267*, 68–77.

Liu, Z., Wang, H., Li, B., Liu, C., Jiang, Y., Yu, G., et al. (2012). Biocompatible magnetic cellulose–chitosan hybrid gel microspheres reconstituted from ionic liquids for enzyme immobilization. *Journal of Materials Chemistry*, *22*, 15085–15091.

Ma, B., Zhang, M., He, C., & Sun, J. (2012). New binary ionic liquid system for the preparation of chitosan/cellulose composite fibers. *Carbohydrate Polymers*, *88*, 347–351.

Ma, H. Y., Hsiao, B. S., & Chu, B. (2011). Thin-film nanofibrous composite membranes containing cellulose or chitin barrier layers fabricated by ionic liquids. *Polymer*, *52*, 2594–2599.

Ma, B., Qin, A., Li, X., & He, C. (2013). High tenacity regenerated chitosan fibers prepared by using the binary ionic liquid solvent (Gly·HCl)-[Bmim]Cl. *Carbohydrate Polymers*, *97*, 300–305.

Muzzarelli, R. A. A. (2010). Chitins and chitosans as immunoadjuvants and non-allergenic drug carriers. *Marine Drugs*, *8*, 292–312.

Muzzarelli, R. A. A. (2011). Biomedical exploitation of chitin and chitosan via mechano-chemical disassembly, electrospinning, dissolution in imidazolium ionic liquids, and supercritical drying. *Marine Drugs*, *9*, 1510–1533.

Pillai, C. K. S., Paul, W., & Sharma, C. P. (2009). Chitin and chitosan polymers: Chemistry, solubility and fiber formation. *Progress in Polymer Science*, *34*, 641–678.

Santos, J. E., Dockal, E. R., & Cavalheiro, E. T. G. (2005). Synthesis and characterization of Schiff bases from chitosan and salicylaldehyde derivatives. *Carbohydrate Polymers*, *60*, 277–282.

Setoyama, M., Kato, T., Yamamoto, K., & Kadokawa, J. (2013). Preparation of chitin/cellulose films compatibilized with polymeric ionic liquids. *Journal of Polymers and the Environment*, *21*, 795–801.

Shih, C. M., Shieh, Y. T., & Twu, Y. K. (2009). Preparation and characterization of cellulose/chitosan blend films. *Carbohydrate Polymers*, *78*, 169–174.

Stefanescu, C., Daly, W. H., & Negulescu, I. I. (2012). Biocomposite films prepared from ionic liquid solutions of chitosan and cellulose. *Carbohydrate Polymers*, *87*, 435–443.

Sun, X., Peng, B., Ji, Y., Chen, J., & Li, D. (2009). Chitosan(Chitin)/cellulose composite biosorbents prepared using ionic liquid for heavy metal ions adsorption. *AIChE*, *55*, 2062–2069.

United States Patent. (2001). *Process for determination of nitrogen, US006287868B1*.

Wu, J., Liang, S., Dai, H., Zhang, X., Yu, X., Cai, Y., et al. (2010). Structure and properties of cellulose/chitin blended hydrogel membranes fabricated via a solution pregelation technique. *Carbohydrate Polymers*, *79*, 677–684.